Nonlinear Theory for Relativistic Plasma Wakefields in the Blowout Regime

W. Lu,[1] C. Huang,[1] M. Zhou,[1] W. B. Mori,[1,2] and T. Katsouleas[3]

[1]*Department of Electrical Engineering, UCLA, Los Angeles, California 90095, USA*
[2]*Department of Physics and Astronomy, UCLA, Los Angeles, California 90095, USA*
[3]*Department of Electrical Engineering, USC, Los Angeles, California 90089, USA*

(Received 22 July 2005; published 26 April 2006)

We present a theory for nonlinear, multidimensional plasma waves with phase velocities near the speed of light. It is appropriate for describing plasma waves excited when all electrons are expelled out from a finite region by either the space charge of a short electron beam or the radiation pressure of a short intense laser. It works very well for the first bucket before phase mixing occurs. We separate the plasma response into a cavity or blowout region void of all electrons and a sheath of electrons just beyond the cavity. This simple model permits the derivation of a single equation for the boundary of the cavity. It works particularly well for narrow electron bunches and for short lasers with spot sizes matched to the radius of the cavity. It is also used to describe the structure of both the accelerating and focusing fields in the wake.

DOI: 10.1103/PhysRevLett.96.165002 PACS numbers: 52.38.Kd, 52.35.Mw, 52.65.Rr

In plasma-based acceleration, a plasma wave with a phase velocity close to the speed of light is driven by a short intense particle or laser beam. When a laser pulse is used it is called laser wakefield acceleration (LWFA) [1] and when a particle bunch is used it is called plasma wakefield acceleration (PWFA) [2]. Most analytical theories to date on plasma waves and wakefield excitation have either been restricted to linear fluid theory [2–4] or one-dimensional nonlinear fluid theory [5,6]. In recent PWFA and LWFA experiments [7,8] the wakes are excited in the so-called blowout regime where electrons are expelled radially. In this regime neither fluid nor one-dimensional (axial) theory applies. These wakes are complicated because their fields are electromagnetic, relativistic mass effects are important, and trajectory crossing occurs.

In the blowout regime all the plasma electrons are expelled from a region around the axis, leaving behind a uniform column of plasma ions. The column is surrounded by a thin layer of the expelled electrons which is surrounded by a weakly perturbed plasma with a thickness of a linear skin depth. The ions pull the electrons back to the axis in about a plasma period (or equivalently a plasma wavelength of $2\pi c/\omega_p$). These electrons overshoot, thereby creating the wake. The first oscillation or bucket is of most interest to plasma-based acceleration. This is illustrated in Fig. 1(a) where the electron density resulting from a short electron bunch is plotted from a fully nonlinear particle-in-cell (PIC) simulation using the code OSIRIS [9]. The electron bunch is propagating to the left in the variable $\xi = ct - z$. The blowout or ion column radius, r_b, is also defined in this plot.

Creating wakefields in the blowout regime was first investigated by Rosenzweig *et al.* [10] for PWFA case of electron beam drivers. These wakefields had perfectly linear focusing fields and had radially independent acceleration fields for electrons. Similar wakefields can be excited by laser drivers. In recent work on LWFA the term bubble regime [11], instead of blowout regime, is used. Despite this intense interest, little theory for how the wakefields in the blowout regime scale with the electron beam or laser beam parameters currently exists; and no theory exists for how beam loading occurs within the ion channel. In addition, while there are expressions for the nonlinear frequency shift [5] for one-dimensional wakes there is no such expression for multidimensional wakes. Recently Barov *et al.* [12], Lotov [13], and Kostyukov *et al.* [14] each have analyzed some aspects of the blowout regime; however, these analyses do not predict the shape of the ion column (bubble) or of the field structures. In this Letter, we will present a predictive theoretical model for wake excitation in the blowout (''bubble'') regime.

We begin with Maxwell's equations in the Lorentz gauge and the equation of motion for a plasma electron.

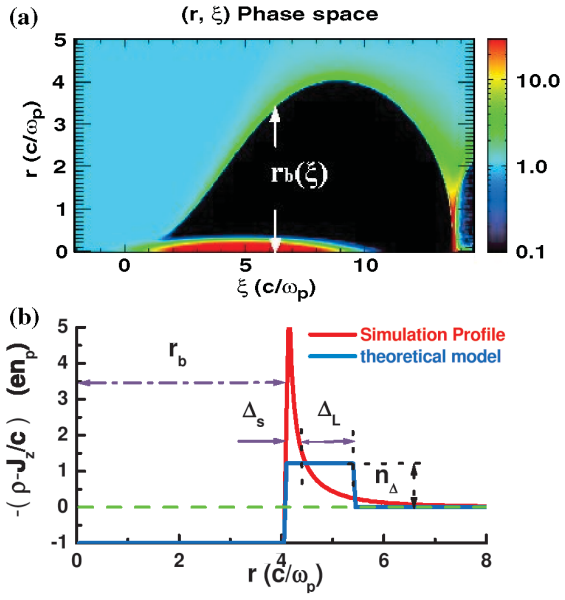

FIG. 1 (color). (a) Electron density with the defined blowout radius $r_b(\xi)$ and (b) $-(\rho - J_z/c)$ profile from a PIC simulation.

For a laser driver, we include the time averaged (over a laser period) ponderomotive force [15]. We transform from the (x, y, z, t) to the $(x, y, \xi \equiv ct - z, s \equiv z)$ variables and make the usual [15] quasistatic or frozen field approximation; i.e., we assume $\partial_s \ll \partial_\xi$ in the field equations. Maxwell's equations then become

$$-\nabla_\perp^2 \begin{bmatrix} \boldsymbol{A} \\ \phi \end{bmatrix} = 4\pi \begin{bmatrix} \boldsymbol{J}/c \\ \rho \end{bmatrix} \tag{1}$$

$$\boldsymbol{\nabla}_\perp \cdot \boldsymbol{A}_\perp = -\frac{\partial \psi}{\partial \xi}, \tag{2}$$

where $\psi \equiv \phi - A_z$, $\boldsymbol{\nabla}_\perp \equiv \hat{\mathbf{x}}\partial_x + \hat{\mathbf{y}}\partial_y$, and $\boldsymbol{A}_\perp = \hat{\mathbf{x}}A_x + \hat{\mathbf{y}}A_y$, etc. Furthermore, it can be shown that the plasma electrons evolve as [15]

$$\frac{d}{d\xi}\boldsymbol{p}_\perp = \frac{1}{c - v_z}\left[-e\left[\boldsymbol{E}_\perp + \left(\frac{\boldsymbol{v}}{c} \times \boldsymbol{B}\right)_\perp \right] - \frac{mc^2}{\bar{\gamma}} \boldsymbol{\nabla}_\perp \frac{|a|^2}{4} \right], \tag{3}$$

where $\bar{\gamma} = (1 + p^2/m^2c^2 + |a|^2/2)^{1/2}$ and the laser field is written as $eA_{\text{laser}}/mc^2 = (a/2)e^{-i\frac{\omega_0}{c}\xi} + \text{c.c.}$ It can also be shown that $\bar{\gamma} - p_z/mc = 1 + e\psi/mc^2$ is a constant of motion [15]. As a consequence of the constant of motion, we can write $p_z/mc = [1 + p_\perp^2/m^2c^2 + |a|^2/2 - (1 + e\psi/mc^2)^2]/[2(1 + e\psi/mc^2)]$ and $\bar{\gamma} = [1 + p_\perp^2/m^2c^2 + |a|^2/2 + (1 + e\psi/mc^2)^2]/[2(1 + e\psi/mc^2)]$. Therefore, $1 - v_z/c = (1 + e\psi/mc^2)/\bar{\gamma} = [2(1 + e\psi/mc^2)^2]/[1 + p_\perp^2/m^2c^2 + |a|^2/2 + (1 + e\psi/mc^2)^2]$ so that once $p_\perp$ and ψ are known so too is the axial momentum. In addition, the pseudopotential ψ obeys the Poisson-like equation,

$$-\nabla_\perp^2 \psi = 4\pi(\rho - J_z/c). \tag{4}$$

Under the quasistatic approximation, the continuity equation becomes $\partial_\xi(c\rho - J_z) + \nabla_\perp \cdot \boldsymbol{J}_\perp = 0$; it then follows that $d[\int(\rho - J_z/c)\boldsymbol{ds}_\perp]/d\xi = 0$. Far in front of the driver where the plasma is unperturbed $\rho - J_z/c = 0$, so $\int(\rho - J_z/c)\boldsymbol{ds}_\perp = 0$ for all ξ. This condition gives ψ a global definition, which is critical for the existence of the constant of motion (see above). In terms of ψ, the axial electric field of the wake, E_z, can be written as

$$E_z = \frac{\partial}{\partial \xi}\psi(\boldsymbol{r}_\perp, \xi). \tag{5}$$

In this way, the wakefield E_z is completely described in terms of ψ, which can be obtained from the Poisson-like Eq. (4) given the source on the right-hand side (RHS). The source term depends on (i) the ion charge density, which is a constant (en_p) for all r, (ii) the charge and current of a narrow sheath formed by the blown-out electrons around $r_b(\xi)$, and (iii) the charge and current of the electrons within a skin depth beyond the narrow sheath. Characterizing the source term in terms of r_b and determining r_b as a function of ξ [via Eq. (11) below] are the central assumption and result of this Letter.

At this point, we will adopt normalized units, where time is normalized to ω_p^{-1}, velocities to the speed of light, c, mass to m, and charge to e. We will begin by assuming the wake is excited by a bi-Gaussian electron driver with a normalized density profile $n_b = [N/(2\pi)^{3/2}\sigma_r^2\sigma_z n_p] \times e^{-r^2/2\sigma_r^2} e^{-\xi^2/2\sigma_z^2}$. We will address how the formalism is modified for a laser driver later. We assume there is azimuthal symmetry and rapidly obtain solutions for Eqs. (1) and (4) because of their Poisson-like form. Inside the ion channel, i.e., for $r \leq r_b$ and for $r \gg \sigma_r$,

$$\phi = \phi_0(\xi) - \frac{r^2}{4} + \lambda(\xi)\ln r \tag{6}$$

$$A_z = A_{z0}(\xi) + \lambda(\xi)\ln r, \tag{7}$$

where $\lambda(\xi) = \int_0^{r \gg \sigma_r} r n_b dr$, $\phi_0(\xi) \equiv \phi(r = 0, \xi)$, $A_{z0}(\xi) \equiv A_z(r = 0, \xi)$, and we assume $j_z = -\text{cen}_b$. In addition, combining the Poisson-like Eq. (1) for A_r with the gauge condition, leads to the relationship $A_r/r = -d_\xi\psi_0/2 = -E_{z0}/2$, for $r \leq r_b$ where $\psi(r, \xi) = \psi_0(\xi) - r^2/4$. If the blown-out electrons form a narrow sheath then the electrons within this layer move nearly tangentially to the ion column boundary. The fact that there is a narrow sheath is confirmed in simulations, e.g., Fig. 1(a). Therefore, the "trajectory" of the boundary, $r_b(\xi)$, can be obtained from the equation of motion for an electron on the boundary. The force on a plasma electron at $r = r_b(\xi)$ or for a beam electron can be written as

$$\begin{aligned} F_\perp &= -(E_r - v_z B_\theta) = \frac{\partial \phi}{\partial r} - v_z \frac{\partial A_z}{\partial r} + (1 - v_z)\frac{\partial A_r}{\partial \xi} \\ &= -\frac{1}{2}r + (1 - v_z)\frac{\lambda(\xi)}{r} - \frac{1}{2}(1 - v_z)\frac{d^2\psi_0}{d\xi^2}r, \end{aligned} \tag{8}$$

where the first term is due to the space charge of the unshielded ion column, and the second and the third terms are due to the electric and magnetic fields from the electron beam and to plasma radial currents, respectively. Note that the focusing force on a beam electron with $v_z \sim 1$ is due only to the space charge of the ion column because the electric and magnetic forces from the plasma currents and the self-forces cancel each other. On the other hand, for plasma electrons for which $-1 < v_z \ll 1$ the force involves the full electromagnetic character of the wake. Inserting Eq. (8) into the equation of motion for a plasma electron [Eq. (3)], $dp_\perp/d\xi = F_\perp/(1 - v_z)$, rewriting the left-hand side as $dp_\perp/d\xi = d[\gamma v_\perp]/d\xi = d[\gamma(1 - v_z)dr_\perp/d\xi]/d\xi = d[(1 + \psi)dr_\perp/d\xi]/d\xi$ [using the constant of motion $\gamma(1 - v_z) = 1 + \psi$], and using the expression for $1 - v_z$ obtained before, the equation of motion for a plasma particle at r_b can now be written as

$$\begin{aligned} \frac{d}{d\xi}\left[(1 + \psi)\frac{d}{d\xi}r_b \right] = r_b\Bigg\{ -\frac{1}{4}\left[1 + \frac{1}{(1 + \psi)^2} + \left(\frac{dr_b}{d\xi}\right)^2 \right] \\ - \frac{1}{2}\frac{d^2\psi_0}{d\xi^2} + \frac{\lambda(\xi)}{r_b^2} \Bigg\}, \end{aligned} \tag{9}$$

where $\psi \equiv \psi[r_b(\xi), \xi] = \psi_0 - r_b^2/4$ is the ψ value along r_b. This equation rigorously describes $r_b(\xi)$ but it is not closed since $\psi_0(\xi)$ is as yet unspecified. In order to get a closed equation for $r = r_b(\xi)$, we need to cast $\psi_0(\xi)$ in

terms of $r_b(\xi)$. Such a relation can be approximately obtained as follows. This is the key simplification in this Letter.

The source term for $\psi(r, \xi)$ is $\rho - J_z$. At each ξ, $\rho - J_z = \rho_{\rm ion} + \rho_e - J_{\rm ze}$, where $\rho_{\rm ion} = 1$ for all r and $\rho_e - J_{\rm ze}$ is zero for $r < r_b$, rises sharply within a sheath of thickness of $\Delta_s(\xi)$ [simulations and analytic arguments [3] show that it is small compared with $r_b(\xi)$ for most of the ion channel, i.e., $\Delta_s/r_b \equiv \epsilon \ll 1$, but its absolute value can be significant, e.g., for $r_b \sim 10$, $\epsilon \sim 0.1$, $\Delta_s \sim 1$] and gradually falls to unity in a width $\Delta_L(\xi)$ [a region where the plasma electrons respond nearly as they would be in a linear wake, $\Delta_L(\xi) \sim 1$ from linear theory]. This is illustrated in Fig. 1(b) where the profile $-(\rho - J_z/c)$ versus r is plotted for an arbitrary value of ξ from Fig. 1(a). $\Delta \equiv \Delta_s + \Delta_L = \epsilon r_b + \Delta_L$ is also defined in Fig. 1(b). The structure of $\rho - J_z$ enables us to write $\psi_0(\xi)$ approximately in terms of $r_b(\xi)$, Δ_L, and ϵ, e.g., $\psi_0(r_b(\xi), \Delta_L, \epsilon)$, by assuming a parametrized profile. We find that very accurate results can be obtained using a very simple profile, which assumes a constant n_Δ over the sheath and the linear region, where $n_\Delta = \frac{r_b^2}{(r_b+\Delta)^2 - r_b^2}$ for $r_b < r < r_b + \Delta$. This is illustrated in Fig. 1(b). Interestingly, the results are very insensitive to the forms of the profiles, but obviously, more refined profiles can be used. For this profile,

$$\psi(r, \xi) = \psi_0(\xi) - \frac{r^2}{4} = \frac{r_b^2(\xi)}{4}(1 + \beta) - \frac{r^2}{4} \qquad (10)$$

for $r \le r_b$ where $\beta[r_b(\xi), \Delta_L, \epsilon] = \frac{(1+\alpha)^2 \ln(1+\alpha)^2}{(1+\alpha)^2 - 1} - 1$ and $\alpha \equiv \Delta/r_b = \Delta_L/r_b + \epsilon$.

All the ξ derivatives of β that arise in Eq. (9) can be written as $d_\xi \beta = d_\xi r_b \partial_{r_b} \beta$ under the assumption that Δ_L and ϵ only depend weakly on ξ so we can assume $\partial_\xi \Delta_L \approx 0$ and $\partial_\xi \epsilon \approx 0$. Proceeding in this way Eq. (9) can then be put in the following form after collecting terms,

$$A(r_b)\frac{d^2 r_b}{d\xi^2} + B(r_b) r_b \left(\frac{dr_b}{d\xi}\right)^2 + C(r_b) r_b = \frac{\lambda(\xi)}{r_b}, \qquad (11)$$

where $A(r_b) = 1 + [\frac{1}{4} + \frac{\beta}{2} + \frac{1}{8} r_b \frac{d\beta}{dr_b}] r_b^2$, $B(r_b) = \frac{1}{2} + \frac{3}{4}\beta + \frac{3}{4} r_b \frac{d\beta}{dr_b} + \frac{1}{8} r_b^2 \frac{d^2\beta}{dr_b^2}$, $C(r_b) = \frac{1}{4}[1 + \frac{1}{(1+\frac{\beta}{4} r_b^2)^2}]$.

Recall that once $r_b(\xi)$ is solved for then $\psi(r)$ is known [Eq. (10)] and $E_z(r = 0, \xi) = d\psi_0/d\xi = d[r_b^2(1 + \beta)/4]/d\xi$ is known. We note here that for a laser driver $C(r_b) = \frac{1}{4}[1 + \frac{1 + \frac{a^2}{2}}{(1+\frac{\beta}{4} r_b^2)^2}]$ and the right side of Eq. (11) becomes $-\frac{\frac{d|a|^2}{dr}\frac{1}{4}}{1+\frac{\beta}{4} r_b^2}$, which comes from the laser's ponderomotive force.

We show the accuracy of our model by directly integrating Eq. (11) for a bi-Gaussian electron beam driver. We choose $k_p \sigma_r = 0.1$ and $k_p \sigma_z = \sqrt{2}$ and electron initial positions $r_0 \ll r_m$. In Fig. 2(a), we plot the trajectories of $r_b(\xi)$ for different values of beam charge, i.e., eN, and hence different maximum blowout radius (r_m varies from 0.18 to 4) and compare these trajectories with the blowout boundaries extracted from fully nonlinear PIC simulations. The theory and PIC simulation results for r_b are essentially identical for each case. We used $\Delta_s = 0.1 r_b$ and $\Delta_L = 1$ for each case. Varying Δ_L from 0 to 3 leads to only a 20% deviation in both the blowout radius and the ion channel length.

Figure 2(b) compares the wakefields, E_z, calculated from the model with those from PIC simulations. The agreement is also excellent until near the rear of the blowout region. We have determined that much of the disagreement comes from assuming constant Δ_s/r_b and Δ_L, which is not exactly true near the rear of the first bucket. In Fig. 2(b) (1), we also plot the wakefield which is calculated using a Δ_L which depends on ξ. This gives better agreement near the rear of the ion column. Although this simple model cannot give exact predictions for E_z near the very rear of the ion channel, it provides the correct trajectory for r_b and hence the correct structure of the wakefield, e.g., the peak decelerating field, the useful accelerating field, the useful transformer ratio, and the wake's wavelength for arbitrary shaped bunches. It also describes quantitatively how the wakefield's structure changes as r_m increases. We also note that it is accurate enough to treat the beam loading problem. Figure 2(b) (2) shows the agreement between the theory and simulation where a drive beam and a trailing beam are used. The agreement is exact within the trailing beam. More details on beam loading will be given in a separate publication.

Much can be learned by examining Eq. (11) in two distinct regimes: namely, the nonrelativistic blowout re-

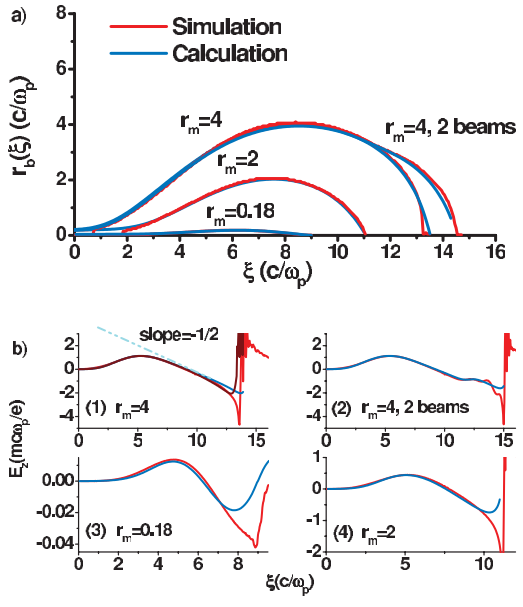

FIG. 2 (color). (a) comparison of the trajectories of $r_b(\xi)$ (beam center is at $\xi = 5$); (b) comparison of the accelerating field $E_z(\xi)$: PIC simulation (red), calculation by a constant profile (blue), calculation by a varying profile (brown, $\Delta_L = 1$ for ξ from 1 to 8, and decreases linearly to 0.2 at $\xi = 15$).

gime where $r_m \ll 1$ and the ultrarelativistic blowout regime where $r_m \gg 1$. In the first limit, connection to the linear fluid can be made, and this will be described in a longer paper. In the ultrarelativistic limit where $r_m \gg 1$, $\beta \ll 1$, and $\beta r_m^2 \gtrsim 4$, Eq. (11) reduces to:

$$r_b \frac{d^2 r_b}{d\xi^2} + 2\left[\frac{dr_b}{d\xi}\right]^2 + 1 = \frac{4\lambda(\xi)}{r_b^2}. \tag{12}$$

The driver bunch length is typically much shorter than the nonlinear ion channel length, so we can ignore the driving term on the right-hand side for much of the trajectory. The equation for a circle is $r_b \frac{d^2 r_b}{d\xi^2} + [\frac{dr_b}{d\xi}]^2 + 1 = 0$ while Eq. (12) gives $r_b \frac{d^2 r_b}{d\xi^2} + 2[\frac{dr_b}{d\xi}]^2 + 1 = 0$ with the right-hand side set to zero. Near the top of a circle $dr_b/d\xi \to 0$, so the trajectory $r_b(\xi)$ maps out a circle until the rear of the blowout region. The effect of the ''extra'' $[dr_b/d\xi]^2$ term is to bend the trajectory downward more quickly as $dr_b/d\xi$ becomes large. This is indeed what is observed in Fig. 2(a). We can rewrite the left-hand side of Eq. (12) as $\frac{d}{d\xi}[\frac{1}{2} r_b \frac{dr_b}{d\xi}] = -\frac{1}{2} - \frac{1}{2}[\frac{dr_b}{d\xi}]^2$, and since $E_z(\xi) \approx \frac{1}{2} r_b \frac{dr_b}{d\xi}$ when $\beta(\xi)$ can be neglected for $r_b \gg 1$, we see that E_z has a slope $\partial_\xi E = -1/2$ at the top of the channel and the slope increases as $dr_b/d\xi$ increases leading to the characteristic spike. This is seen in Fig. 2(a) where a line with a slope of $-1/2$ is shown for convenience.

For most situations of interest, the driver is sufficiently short that at the point where $r_b(\xi_0) = r_m$ the right-hand side of Eqs. (11) and (12) can be neglected. For $\xi > \xi_0$ and for $r_m \gtrsim 4$ the trajectory for r_b maps out a circle and the ion column is a sphere, i.e., a bubble. The value of $E_z = 0$ at $\xi = \xi_0$, and E_z decreases linearly from 0 to $-r_m/2$ in a distance $L_c = r_m$. Therefore, the nonlinear frequency or wave number is $\omega_{\rm NL} = \frac{\pi}{r_m}\omega_p$ and in term of the amplitude $E_{z\max} = r_m/2$, $\omega_{\rm NL} = \frac{\pi}{2E_{z\max}}\omega_p$. Interestingly, the same relationship holds for nonlinear one-dimensional plasma oscillations [5] although the physics is completely different. In these 3D wakes the wakefields are electromagnetic in character. Besides the accelerating axial electric field, E_z, there are transverse electric, E_r, and magnetic fields, B_θ. The E_r fields come from the ion column, $E_{r\rm ion} = r/2$, and the radial plasma current, $E_{r\rm EM} = -r/4$ while B_θ comes from the radial plasma current, $B_{\theta\rm EM} = -r/4$. The total focusing field on a beam electron is $E_r - B_\theta = r/2 = E_{r\rm ion}$.

We conclude by describing the differences between wake excitation by short ($\omega_p \tau \lesssim 1$) electron and laser drivers. For the electron driver case, the bunch is typically narrow, $\sigma_r \ll r_m$, and the ultrarelativistic limit is generally not reached. For example, in the E164X experiments [8], $N = 1.8 \times 10^{10}$, $\sigma_z = 30\ \mu$m, $\sigma_r = 10\ \mu$m, and the plasma density was 5×10^{16} cm^{-3}. Therefore, $n_b/n_p \approx 7$ and $\lambda(\xi) \approx 1$. To estimate r_m, we use Eq. (11) and solve for the equilibrium radius, $r_{\rm eq}$, by dropping the first two terms in the left-hand side. The value of $r_m \approx 2r_{\rm eq}$ [3] which is $\approx$2 for this case. On the other hand, narrow lasers ($W_0\omega_p/c \ll 1$) cannot be guided and unlike the space charge force of an electron beam, the ponderomotive force only extends out to the edge of the laser. Simulations show that the best defined sheaths are generated when $W_0 \sim r_m$. Under this condition, electrons at an initial radius near W_0 will experience an impulse before the ion channel forces have fully developed. These electrons then move outward until the ion channel force brings it to rest. For other values of W_0 the simple sheath model [Fig. 1(b)] does not work as well. One can estimate r_m by balancing the ion channel force by the ponderomotive force in vacuum leading to $r_m \sim 2\sqrt{a_0}$ [14,16,17]. The ultrarelativistic limit, $r_m \gtrsim 4$, can be reached when $a_0 \gtrsim 4$ and $W_0 \sim r_m \sim 2\sqrt{a_0}$, which requires a laser power $P = [a_0^2 W_0^2/32]P_c \sim 8P_c$ where P_c is the critical power for relativistic self-focusing [16]. For current state-of-the-art lasers [7,18], $15 \lesssim P \lesssim 100$ TW, reaching the ultrarelativistic blowout (bubble) regime requires the use of plasma densities between $2 \times 10^{19} \gtrsim n_p \gtrsim 2 \times 10^{18}$ cm^{-3}, respectively.

This work is supported by DOE under Grants No. DE-FG02-03ER54721, No. DE-FG03-92ER40727, and No. DE-FG03-92ER40745.

[1] T. Tajima and J. M. Dawson, Phys. Rev. Lett. **43**, 267 (1979).
[2] P. Chen *et al.*, Phys. Rev. Lett. **54**, 693 (1985).
[3] W. Lu *et al.*, Phys. Plasmas **12**, 063101 (2005); the special issue of Phys. Plasmas (to be published).
[4] E. Esarey *et al.*, IEEE Trans. Plasma Sci. **24**, 252 (1996), and references therein; L. M. Gorbunov and I. I. Kirsanov, Sov. Phys. JETP **66**, 290 (1987).
[5] A. I. Akhiezer and R. V. Polovin, JETP (U.S.S.R.) **30**, 915 (1956).
[6] J. M. Dawson, Phys. Rev. **113**, 383 (1959).
[7] S. P. D. Mangles *et al.*, Nature (London) **431**, 535 (2004); C. G. R. Geddes *et al.*, Nature (London) **431**, 538 (2004); J. Faure *et al.*, Nature (London) **431**, 541 (2004).
[8] M. Hogan *et al.*, Phys. Rev. Lett. **95**, 054802 (2005).
[9] R. Fonseca *et al.*, *Lecture Notes in Computer Science* (Springer, Heidelberg, 2002), Vol. 2329, III-342.
[10] J. B. Rosenzweig *et al.*, Phys. Rev. A **44**, R6189 (1991).
[11] A. Pukhov and J. Meyer-ter-vehn, Appl. Phys. B **74**, 355 (2002).
[12] N. Barov and J. B. Rosenzweig, Phys. Rev. ST Accel. Beams **7**, 061301 (2004).
[13] K. V. Lotov, Phys. Rev. E **69**, 046405 (2004).
[14] I. Kostyukov *et al.*, Phys. Plasmas **11**, 5256 (2004); S. Gordienko and A. Pukhov, Phys. Plasmas **12**, 043109 (2005).
[15] P. Mora and T. M. Antonsen, Jr., Phys. Plasmas **4**, 217 (1997).
[16] Guo-Zheng Sun *et al.*, Phys. Fluids **30**, 526 (1987).
[17] We inferred the coefficient of two from simulations.
[18] F. S. Tsung *et al.*, Phys. Rev. Lett. **93**, 185002 (2004).